Temperature-dependent EPR for the ferrous impurity in $KMgF_3$

H. Kim and J. Lange
Department of Physics, Oklahoma State University, Stillwater, Oklahoma 74074
(Received 1 December 1977)

Several unusual features of the electron paramagnetic resonance spectrum for the ferrous ion in $KMgF_3$ are observed as a function of temperature. Superhyperfine (SHF) interactions between the ferrous ion and the nuclear spin of its fluoride neighbors ($I = 1/2$) are observed and analyzed using an effective spin Hamiltonian which yields the hyperfine-coupling tensor components ($T_\parallel = 160$ MHz, $T_\perp = 80$ MHz). The SHF spectrum is observed for both doublet transitions ($\Delta M_s = 2$) and double-quantum singlet ($\Delta M_s = 1$) transitions. The height of the double-quantum transitions exhibits an unusual dependence on the microwave power. The temperature dependence of the height of the double-quantum transitions is also a function of the microwave power. At intermediate temperatures ($T > 10$°K) SHF lines of inverted phase are observed. A model employing self-cross-relaxation of single-ion spin packets ($\Delta M_s = 1$) is applied to fit the temperature dependence of the inverted SHF lines numerically. Finally, the behavior of the complete spectrum is observed for high-impurity concentrations of ferrous ions where orthorhombic strain effects become dominant and there are the initial vestiges of evanescent ordering at the lowest temperatures.

I. INTRODUCTION

The ferrous ion in octahedral crystal fields exhibits features associated with the dynamic Jahn-Teller effect as well as some unusual Zeeman transitions. In this investigation the ferrous ion is a substitutional impurity for magnesium in $KMgF_3$. The lower-energy electronic states issue from the spin-orbit splitting of the $^5T_{2g}$ term. The resulting ground state is a triplet T_{2g} with the first excited states being a closely spaced doublet E_g and triplet T_{1g}. Crystal-field theory predicts these excited states to be ~195 cm^{-1} above the ground-state triplet but the dynamic Jahn-Teller effect and covalency reduce[1] this value. Based on measurements of the g factor and temperature dependence of the absorption width, an upper bound on the Jahn-Teller energy of 108 cm^{-1} is obtained ignoring covalency. This dynamic Jahn-Teller effect leads to a significant reduction in the spin-orbit ground-state splitting compared to the crystal-field prediction of ~195 cm^{-1}. The observed value of 95 cm^{-1} (determined from the temperature dependence of the linewidth[2]) is compatible with the value calculated from spin-orbit coupling reduced by the dynamic Jahn-Teller effect ($E_{JT} = 108$ cm^{-1}).

In this investigation various features of the paramagnetic behavior of the ferrous ion in octahedral coordination with six fluoride ions are considered. The interaction between the magnetic moment of the ferrous ion and the nuclei of the fluoride neighbors ($I = \frac{1}{2}$) leads to a superhyperfine (SHF) interaction. This interaction is analyzed employing an effective spin Hamiltonian.

The (SHF) interaction is not only observed for single-photon Zeeman transitions, but also for "simultaneous" two-photon transitions. These latter double-quantum (DQ) transitions are observed to decrease rapidly as a function of temperature. At higher temperatures features appear in the spectra which yield derivatives of inverted phase. One mechanism for these inverted-phase transitions has been suggested by Smith, Dravieks, and Wertz[3] as being due to "self-cross-relaxation" between overlapping spin packets. This model is used to analyze the temperature dependence of the SHF-inversion-line spectrum to yield the self-cross-relaxation time.

Finally, we will consider the dependence of the linewidth and position on the impurity concentration. As the ferrous impurity concentration increases, the absorption spectrum broadens and the centers of various spectral features shift relative to one another.

II. PARAMAGNETIC RESONANCE SPECTRA WITHIN THE GROUND STATE

The electronic ground state of the ferrous ion is triply degenerate in a cubic crystal field. Although the field is cubic for the magnesium site in the perfect host $KMgF_3$ lattice, it is likely that imperfections and impurities lead to an inherent strain distribution in the host lattice. Linear strains which reduce the cubic site to a tetragonal symmetry remove part of the ferrous electronic ground-state degeneracy leading to a singlet and doublet separated by an energy proportional to the tetragonal strain magnitude. A further reduction in the degeneracy of the doublet occurs if the linear strains lead to an orthorhombic distortion of the site. The effect of these linear distortions is illustrated in Fig. 1. The zero-field splitting of the ground-state electronic triplet (which is

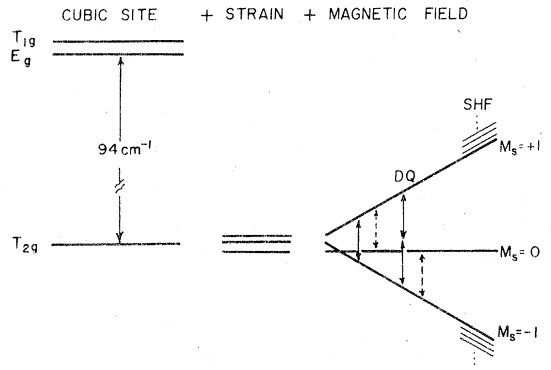

FIG. 1. First excited states of the ferrous ion are 94 cm^{-1} above the T_{2g} ground state due to a spin-orbit interaction quenched by the dynamic Jahn-Teller effect. Lattice strains lead to local tetragonal (e_θ) and orthorhombic (e_ϵ) distortions at the ferrous site which further reduce the degeneracy of the ground-state triplet (T_{2g}). Application of a magnetic field further splits the ground state with transitions between $M_s=0$ and $M_s=\pm1$ (dashed lines) separated along the magnetic field axis proportional to the local strain. The added perturbation due to the six neighboring fluoride ions further splits the $M_s=\pm1$ levels and SHF structure is observed.

less than 0.5 cm^{-1} in this investigation) contributes to the broadening of the EPR line. Strains introduced in the crystallization process are likely to be distributed over a range of values resulting in a distribution of zero-field splitting and a range of effective g values. Each impurity site can be thought of as contributing a "spin-packet" to the total line shape. The spin packet has an effective g value dependent on the zero-field splitting of the ground-state triplet of the ferrous ion. The width of the spin packet is related to the intrinsic spin-lattice relaxation (T_2) and nuclear broadening due to the fluoride neighbors. This width is considerably less than the observed linewidth which has contributions from all the spin packets whose effective g values are distributed over values which depend on the magnitude and symmetry of the local strain.

Application of an external magnetic field removes any remaining degeneracy of the ground-state triplet and it splits into three electronic levels labeled by $M_s=0,\pm1$. In a strictly cubic field, transitions between $M_s=0$ and $M_s=\pm1$ ($\Delta M_s=1$) are allowed and are usually observed as a broad line whose width reflects primarily the tetragonal strain components. For lower than cubic symmetry $M_s=+1$ to $M_s=-1$ transitions become allowed with a linewidth related to the orthorhombic strains. These latter transitions ($\Delta M_s=2$) usually yield narrower lines than the $\Delta M_s=1$ transitions. In addition to these two transitions involving single-quantum absorption, there are double-quantum absorptions between the $M_s=+1$ and $M_s=-1$ levels.

Although these three features lead to a rather complicated spectrum in themselves, there is an additional interaction between the ferrous ion and the $I=\frac{1}{2}$ nuclear spin of the six fluoride nearest neighbors. This futher splits the $\Delta M_s=2$ transitions (both normal and double quantum) into at least seven lines. Depending on the direction of the magnetic field and the relative positions of the fluoride ions and ferrous impurity the prominant SHF lines are for $\Delta M_I=0$ nuclear transitions while smaller $\Delta M_I=1$ "forbidden" transitions are also observed. A representative spectrum is shown in Fig. 2 with the minimum number of SHF lines present for six fluoride neighbors. ($\vec{H}\parallel[111]$). The SHF splitting of the $\Delta M=2$ transitions is observed at low temperatures (< 17 °K) while the double quantum SHF is observed only with higher powers.

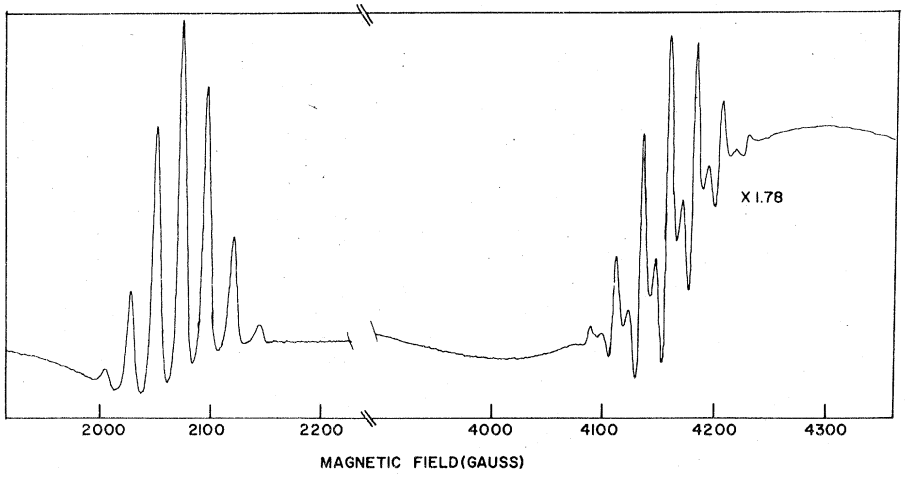

FIG. 2. Derivative spectrum of the ferrous ion showing the SHF splitting of the $\Delta M_s=2$ and double-quantum transitions. The $KMgF_3$ host material contains a low level of iron impurities (30 ppm) and exhibits a minimum of lattice strain which is reflected in the relatively narrow (~250 0G) $\Delta M_s=1$ transition. The measurement frequency is 20 GHz at a temperature of 4.2 °K.

III. SUPER-HYPERFINE SPLITTINGS

The interaction of the ferrous electronic moment with the nuclear moments of the neighboring fluoride ions can be expressed in terms of an effective spin Hamiltonian given by

$$H = g\mu_B \vec{H}\cdot\vec{S} + \sum_{i=1}^{6}(\vec{S}\cdot\vec{\vec{T}}\cdot\vec{I}_i - g_n\mu_n\vec{H}\cdot\vec{I}_i). \quad (1)$$

The first term is the Zeeman splitting of the ferrous electronic state. The second term reflects the interaction of the ferrous magnetic moment with the nuclear moments ($\vec{I}_i$) of the fluoride ions through the hyperfine coupling tensor $\vec{\vec{T}}$. The final term is the Zeeman splitting of the nuclear state in an external field $\vec{H}$.

As seen in Fig. 2, a series of lines due to SHF interactions appears in two positions. The six fluoride nearest neighbors are in equivalent sites when the external magnetic field is along the [111] crystallographic direction. The theoretical SHF structure consists of seven equally spaced lines with an intensity ratio of 1 : 6 : 15 : 20 : 15 : 6 : 1 for $\Delta M_I = 0$. This theoretical SHF spectrum is consistent with two features seen in Fig. 2. The series of low-field lines are spread around a position corresponding to a $\Delta M_s = 2$ electronic transition. The second set of SHF lines appears at the center of the strain broadened $\Delta M_s = 1$ transition. This second feature is attributed to double-quantum absorptions between the $M_s = \pm 1$ levels. The intensities of these lines are observed to have both an anomalous temperature and power dependence and will be considered separately in a later section.

The $\Delta M_s = 2$, SHF lines appearing at the lower magnetic field have a central peak which yields a g factor of 3.440 ± 0.0005. This value is substantially larger than previously reported[4] and agrees, within experimental uncertainty, with the value obtained from the center of the strain broadened $\Delta M_s = 1$ peak and the double-quantum SHF lines. To find the SHF coupling tensor $\vec{\vec{T}}$ we can relate the observed SHF splitting ΔH^i by the fluorine nuclear spin to the tensor components $|T_\parallel|$ and $|T_\perp|$ in the principal axis coordinate system by

$$(g\mu_B \Delta H^i)^2 = T_\perp^2 + (T_\parallel^2 - T_\perp^2)\cos^2\phi\,, \quad (2)$$

where ϕ is the angle between the external field and the principal (crystal) axis direction.[5] When the external field is aligned to [111] direction the d electron experiences six equivalent fluorine nuclear spins. For this field direction we observe seven SHF lines spaced equally by 23 G with $\phi = 55°$. When the external field is along [100] we have four equivalent fluorines with $\phi = 90°$ and two equivalent fluorines with $\phi = 0°$. The observed SHF shows nine equivalent intervals of 16.5 G. This is expected for this field direction if we assume that the two fluorines with $\phi = 0°$ give twice as much splitting as the fluorine with $\phi = 90°$. Taking $g = 3.440$ and using (2) both for [100] and [111] directional magnetic fields we find $|T_\parallel| = 160$ MH$_z$ and $|T_\perp| = 80$ MH$_z$.

In addition to the seven line hyperfine spectrum which appears in Fig. 2, there is an additional six line component observed for the DQ SHF appearing between the seven lines. These six lines are from the so-called "forbidden transitions" where $\Delta M_I = 1$. These occur because the resultant magnetic field at the fluoride site is not parallel to the external field due to the addition of the magnetic field of the ferrous d-electron spin states. Consequently the nuclear-spin states will not be orthogonal to the d-electron spin directions causing a nonconservation in total nuclear spin in the electronic state transitions. The intensity and position of these forbidden transitions is often used to determine the signs of $T_\parallel$ and $T_\perp$. For the DQ SHF structure a degree of caution must be exhibited since the available intensity expressions are derived for single-quantum transitions. With this caution in mind one can apply the expressions of Clogston *et al.*[6] to the double-quantum process. Of the two choices of signs for $T_\parallel$ and $T_\perp$ the one which gives the largest intensity (4%) and the closest to the observed values (10%) is for opposite signs. It also explains why no appreciable "forbidden transitions" appear for the $\Delta M_s = 2$ single-quantum transitions at lower fields where the calculated intensity would be only 0.5%. Although one normally expects two "forbidden transitions" between each SHF line, the values of $T_\parallel$ and $T_\perp$ for this system lead to an overlap of these lines. The different signs of $T_\parallel$ and $T_\perp$ indicate no appreciable overlap of S-type orbitals (Fermi contact) at the fluorine site.[7] A minimum covalency might be implied from this result which is consistent with the assumptions made in calculating the dynamic Jahn-Teller reduction parameters.

IV. DOUBLE-QUANTUM ABSORPTION

The "simultaneous" absorption of two microwave photons to induce a transition between the $M_s = -1$ and $M_s = +1$, using two different quanta states has been observed directly by Orton, Auzins, and Wertz.[8] In this investigation the double-quanta features occur as SHF lines located at the center of the $\Delta M_s = 1$ transition. The intensities and relative positions of these lines leave no doubt they involve transitions between the nuclear split

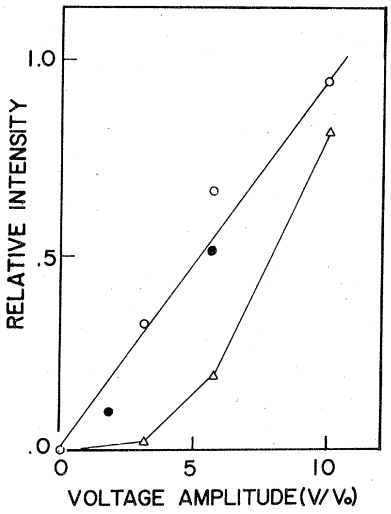

FIG. 3. Relative intensity of various EPR transitions as a function of microwave drive voltage. The $\Delta M_s = 1$ (0) and $\Delta M_s = 2$ (0) transitions are linear with microwave drive voltage while the double-quantum features vary as its cube. The specimen has low-impurity concentration (30 ppm) and is observed at a frequency of 20 GHz and a temperature of 4.2 °K.

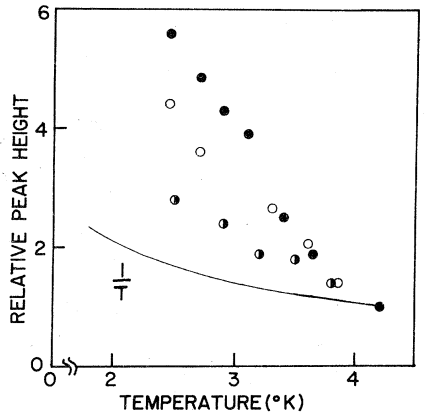

FIG. 4. Peak height of the double-quantum transitions in the low-concentration sample as a function of temperature. The peak height is normalized to unity at 4.2 °K and varies with microwave power (◑, 1 mW; ○, 0.32 mW; ●, −0.18 mW). The solid curve is proportional to $1/T$.

$M_s = \pm 1$ levels. The position of the center of the SHF lines at the exact center of the single-quantum $\Delta M_s = 1$ transition demonstrates that a two quantum absorption is necessary to induce the $\Delta M_s = 2$ transition.

The relative positions of the components of this SHF feature are the same as those observed at lower fields due to single-quantum $\Delta M_s = 2$, $\Delta M_I = 0$ absorption. The linewidths of the DQ SHF feature are somewhat smaller (~20% less) than the lower field SHF spectrum, and an additional set of smaller lines appear due to so called "forbidden transitions" ($\Delta M_I = 1$) as discussed previously. Two interesting features of the DQ SHF spectrum are manifested in an unusual power and temperature dependence of the spectrum. The narrow width of the DQ SHF lines facilitates an accurate determination of the dependence of the spectrum on both microwave power and temperature.

The power dependence of the DQ features have been observed previously for transition-metal ions in various hosts.[9] For the ferrous ion in $KMgF_3$ the power dependence intensity of the low field ($\Delta M_s = 2$) SHF structure and $\Delta M_s = 1$ strain broadened features are compared with that of the DQ SHF lines in order to establish the power dependence of the detection system ($T = 4.2$ °K). Both the intensity of the low-field SHF spectrum and $\Delta M = 1$ transitions are observed to be linear with microwave drive voltage (square root of the power) as would be expected (Fig. 3). The DQ SHF intensity is seen to be dependent on the cube of the voltage (the three halves power of the microwave power). The ratio of the intensity of the allowed to forbidden DQ SHF lines is observed to decrease slightly with increasing power.

The intensity of the DQ SHF spectrum is very sensitive to temperature. All the "normal" double-quantum features disappear from the spectrum at temperatures above 10 °K even at high microwave powers (<1mW). The low-temperature behavior of the DQ SHF intensity is observed to be more rapid than the $\sim 1/T$ behavior characteristic of excitation from a ground state (the $\sim 1/T$ intensity behavior is observed for both the $\Delta M_s = 1$ line and the low-field $\Delta M_s = 2$ SHF lines). The intensity of the DQ SHF lines is observed to decrease in a complicated manner (Fig. 4) with the lower microwave powers exhibiting a more rapid decrease in intensity as a function of temperature. At the lowest powers the decrease is proportional to $1/T^3$. The transition probability for the DQ absorption appears to be related to the density of photons through the microwave power while the temperature dependence of the intensity also indicates a dependence on the lifetime of the states.

V. INVERSION LINE

The normal DQ SHF spectrum decreases in intensity rapidly with increasing temperature and is replaced ($T > 10°$) by a spectrum which exhibits a SHF derivative of inverted phase. This means that superimposed on the broad $\Delta M_s = 1$ absorption peak are a series of sharp *decreases* in the absorption at the position of the SHF lines (Fig. 5). Since these inverted features appear at the same

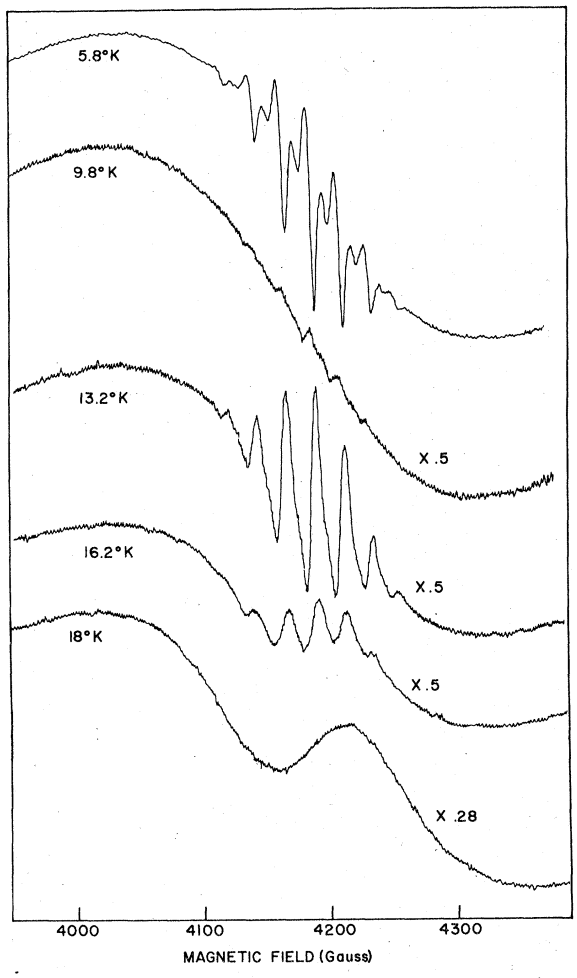

FIG. 5. Derivative spectrum of the ferrous ion in low concentration showing the change from SHF spectrum caused by double-quantum transitions to inverted lines (13.2°K). Thermal broadening obliterates the SHF structure at higher temperatures and leaves only a single inverted line.

position as the SHF spectrum and do *not* exhibit the anomalous power dependence of the DQ SHF lines, they indicate transitions between the nuclear split $M_s = \pm 1$ levels but *not* by two quantum absorption. These transitions appear to be single-quantum transitions involving $\Delta M_s = 1$. What distinguishes them from the strain broadened ($\Delta M_s = 1$) features of normal phase discussed previously, is the small width of the lines, their inverted phase, and the appearance of SHF structure. A mechanism suggested by Smith, Dravnieks, and Wertz[3] can account for these features. They propose a self-cross-relaxation mechanism between spin packets of a single atom. The self-cross-relaxation can only occur when the ($\Delta M_s = 1$) spin-packets of a single atom overlap; i.e., the strain at that atomic site is not large enough to shift the ($\Delta M_s = 1$) spin packets more than their half width from each other. This qualitatively explains why the inversion lines are narrow compared to the normal $\Delta m = 1$ transition. Only those atoms for which the strain is small enough that the narrow spin packets overlap are then capable of participation in a self-cross-relaxation transition.

The intensity of the $\Delta m = 1$ transition, including the inversion line, was derived by Smith, Dravnieks, and Wertz using a density matrix technique. At low powers, the intensity is given by

$$I \propto \frac{W + 1/T_2}{\delta^2 + (W + 1/T_2)^2} + \frac{1}{W T_2^*}\left(\frac{W + 1/T_2}{\delta^2 + (W + 1/T_2)^2} - \frac{1/T_2}{\delta^2 + (1/T_2)^2}\right), \quad (3)$$

where the first term is the normal $\Delta M_s = 1$ line and the difference in the second term leads to the inversion line. The center frequency of the spectrum is given by ω_0 where $\delta = \omega_0 - \omega$, the width of the strain broadened $\Delta M_s = 1$ transition is W while the individual spin-packet width is proportional to $1/T_2$ and is taken as the width of the SHF lines.

The intensity of the inversion line is dependent on the widths of the spin packets which vary with temperature. The spectrum shown in (Fig. 5) includes both the normal $\Delta M_s = 1$ strain broadened line and the inversion line SHF spectrum. The height of the inversion SHF spectrum changes considerably with temperature exhibiting a maximum (Fig. 6) and eventually merges into a broadened feature (the overlapping SHF lines). The strain-broadened $\Delta M_s = 1$ line intensity changes little in this temperature range and varies as $1/T$. Qualitatively, the inversion line temperature dependence can be ascribed to the variation of the width of the spin packets. At low temperatures the spin packets are very narrow and probably limited by nuclear broadening. As the temperature increases, indirect transitions to higher spin-orbit split levels (~94 cm^{-1}) lead to an Orbach broadening. As the spin packets broaden, there are more ions for which the ($\Delta M_s = 1$) spin packets overlap and can undergo self-cross-relaxation, thereby increasing the inversion line intensity. At higher temperatures population effects can reduce the number of ions in the ground state, and lead to an overall decrease in intensity. This qualitative explanation can be quantified by fitting the expression [Eq. (3)] for the $\Delta M_s = 1$ strain broadened line and the self-cross-relaxing SHF lines to the data of Fig. 5. At each temperature, Eq. (3) is used to fit the intensity of the normal $\Delta M_s = 1$ line and the inversion line by varying the self-cross-relaxation

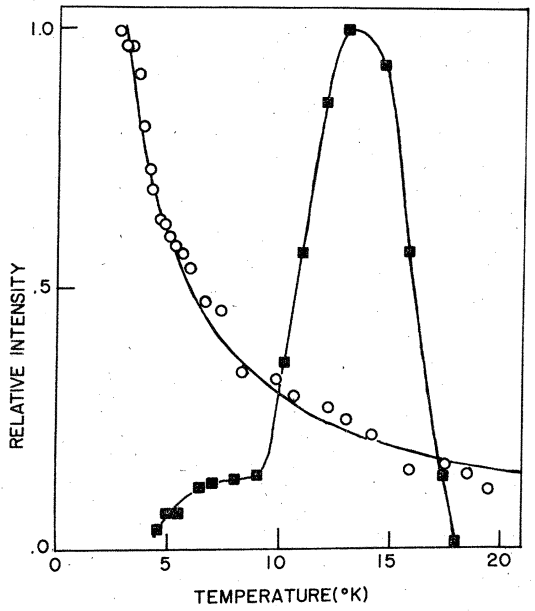

FIG. 6. Relative intensity of the $\Delta M_s = 1$ transition (O) and inverted line as a function of temperature. The curve through the $\Delta M_s = 1$ points (O) is proportional to $1/T$.

time T_2^*. The width of the strain-broadened $\Delta M_s = 1$ transition (W) is determined from the data as is the spin-packet width and the positions of the SHF spectra. The fitting procedure consists of varying the magnitude of the self-cross-relaxtion time T_2^* until the observed intensities are matched. The resulting cross-relaxation time is determined as a function of temperature in the range from 10 to 17 °K, where the inversion intensity is a maximum (Fig. 6). The effective self-cross-relaxation overlap (ΔH) of the spin packets is, approximately 0.1 G at 10 °K and can be fitted with an expression $\Delta H = 409e\text{-}88/T$. The small spin-packet overlap causes the intensity of the inversion lines to be much less than for normal $\Delta M_s = 1$ transitions. Only those ions in sites with strains less than 10^{-6} have the necessary overlap of spin packets to facilitate the self-cross-relaxation. In samples with higher impurity concentration and an accompanying increase in strain, the inversion line is observed but no SHF structure is seen. Orthorhombic strains appear to shift the $M_s = \pm 1$ levels and smear out the SHF structure in a manner similar to the thermal broadening seen in Fig. 5.

VI. HIGHER CONCENTRATIONS OF FERROUS IMPURITY

As the ferrous impurity concentration increases beyond 35 ppm, the EPR spectrum broadens. Although three major features still remain (Fig. 7) the lines are spread over a kilogauss range when the impurity concentration reaches 9200 ppm. There is also a notable absence of any superhyperfine structure even at the lowest temperatures.

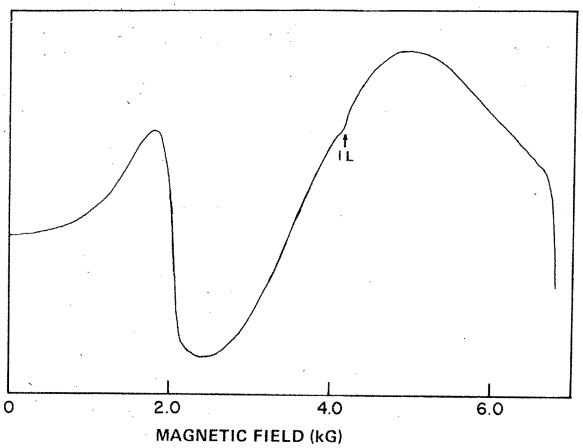

FIG. 7. Derivative of the absorption spectrum for the ferrous ion in a higher-impurity-concentration (9200-ppm) crystal of $KMgF_3$.

The three major features which remain are the normal $\Delta M_s = 1$ line, the inversion line, and the $\Delta M_s = 2$ transition without SHF structure. The linewidths of the first two features are shown as a function of temperature for three impurity concentrations in Fig. 8. The higher concentration samples (4000 and 9200 ppm) exhibit spectra that are so broad that the onset of thermal broadening due to indirect transitions is not observed. The broadening for the higher concentrations likely results from strains introduced by the addition of larger amounts of the impurity. The ground-state triplet of the ferrous ion is split over a wide energy range due to the distribution of lattice

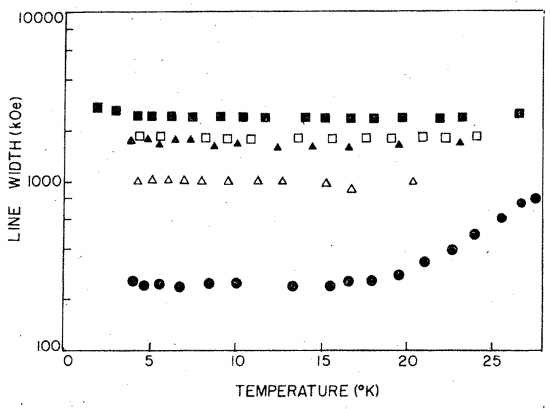

FIG. 8. Linewidths for three different impurity concentrations of ferrous ion (30 ppm, ●; 4000 ppm, Δ; 9200 ppm, □) in $KMgF_3$. The open points are for $\Delta M_s = 1$ transitions while the solid ones are for $\Delta M_s = 2$ transitions. The measurement frequency is 20 GHz.

strains which may vary in both magnitude and symmetry. For the tetragonal (e_θ) strain, the $M_s = 0$ level is shifted relative to the $M_s = \pm 1$ level. The degree of shifting is proportional to the magnetoelastic coupling constant ($G_{11} = 1000\ \mathrm{cm}^{-1}$/unit strain) and the magnitude of the tetragonal strain component. The tetragonal lattice strain distributions lead to a broadening of the $\Delta M_s = 1$ line and the linewidth then reflects the order of magnitude of strain acting on an average impurity site. A strain magnitude of $\sim 10^{-4}$ is determined from the width of the 9200-ppm sample.

An interesting feature of the spectrum of Fig. 7 are the relative positions of the derivatives and their effective g factors. The g factor for the three features of interest are identical when the strains are very low. As can be seen in Fig. 7 the position of the center of the $\Delta m = 1$ line and the inversion line do not coincide as is observed for the lower impurity concentration (Fig. 2). The magnitude of the g factor for the inversion line, however, is the same in the high- and low-concentration samples since only impurities in sites where the strain shift of the spin packets is smaller than their width can exhibit the self-cross-relaxation. Therefore, impurities experiencing a minimum of strain are the only ones which contribute to the inversion line regardless of the impurity concentration and thus reflect the common g factor for the almost unstrained ($\sim 10^{-6}$) site.

The shift of the center of the $\Delta M_s = 1$ line to higher effective g factors requires strains other than tetragonal. For purely tetragonal strains the width of the line but not its position can be affected since only the $M_s = 0$ level is shifted relative to the $M_s = \pm 1$ levels. For orthorhombic strains the three levels $M_s = 0, \pm 1$ are shifted relative to each other. The shift of the $M_s = +1$ and $M_s = -1$ levels away from each other would lead to a larger effective g factor in addition to broadening the resonance peak. A shift of the center of the line to higher g factors suggests an orthorhombic strain distribution which is centered about some nonzero strain value.

At the lowest temperature (<5 °K) the higher-concentration samples exhibit unusual behavior in both the peak width and g factor. For the highest-concentration sample (9200-ppm Fe^{2+}) the peak width is constant over a wide temperature range and interpreted as due to strain broadening. However, there is a linewidth increase of about 15% between 5 and 2.5 °K. Above 5 °K the width is constant to over 30 °K (Fig. 8). The effective g factor also decreases below 5 °K by approximately 2%. Both these observations suggest the initial onset of ordering below 5 °K. This is not to suggest a magnetic phase transition occurs but rather an onset of critical fluctuations due to evanescent phase coherence between the motion of the ferrous spins. Similar behavior has been observed in the acoustic attenuation at the lower temperatures and will be considered elsewhere.[11]

VII. SUMMARY AND CONCLUSIONS

The SHF tensor components have been evaluated for the ferrous ion in $KMgF_3$. From the magnitude of the "forbidden" transitions the signs of the hyperfine tensor components are implied and are shown to indicate small S state overlap with the fluoride neighbors. The observation of SHF structure for the ferrous ion also facilitates determination of the temperature dependence of various exotic EPR features such as double-quantum transitions and inversion lines. This latter feature is interpreted quantitatively using a self-cross-relaxation model between strain-shifted spin packets. The constancy of the inversion line position even in specimens with larger strain (increasing impurity concentration) results only from ions in low strain sites. For the highest-impurity concentration sample, there is an increase in line width as the temperature decreases suggesting the onset of critical fluctuations as a precursor to magnetic ordering.

Note added in proof. Recent measurements of the superhyperfine parameters at 35 GHz by Galindo, Owen, and Murrieta[12] are in agreement with the above results.

ACKNOWLEDGMENT

This work was supported in part by the NSF.

[1] F. Ham, W. Schwarz, and M. O'Brien, Phys. Rev. 185, 548 (1969).
[2] H. Kim and J. Lange, Phys. Rev. Lett. 39, 501 (1977).
[3] S. Smith, F. Dravnieks, and J. Wertz, Phys. Rev. 178, 471 (1969).
[4] J. Vallin and W. Piper, Solid State Commun. 9, 823 (1971).
[5] J. Hall and R. Schumacher, Phys. Rev. 127, 1892 (1962).
[6] A. Clogston, J. Gordon, V. Jaccarino, M. Peters, and L. Walker, Phys. Rev. 117, 1222 (1960).
[7] U. Ranon and J. Hyde, Phys. Rev. 141, 259 (1966).
[8] J. Orton, P. Auzins, and J. Wertz, Phys. Rev. Lett. 4, 128 (1960).
[9] D. McMahon, Phys. Rev. 134, A128 (1964).
[10] J. Combay, thesis (The University of Grenoble, Grenoble, 1976) (unpublished).
[11] H. Kim and J. Lange (unpublished).
[12] S. Galindo, J. Owen, and H. Murrieta, J. Phys. C 11, L73 (1978).